

Mixed-feedback oscillations in the foraging dynamics of arboreal turtle ants

Alia Valentine, Deborah M. Gordon, Anastasia Bizyaeva

Abstract—We propose and analyze a model for the dynamics of the flow into and out of a nest for the arboreal turtle ant *Cephalotes goniodontus* during foraging to investigate a possible mechanism for the emergence of oscillations. In our model, there is mixed dynamic feedback between the flow of ants between different behavioral compartments and the concentration of pheromone along trails. On one hand, the ants deposit pheromone along the trail, which provides a positive feedback by increasing rates of return to the nest. On the other hand, pheromone evaporation is a source of negative feedback, as it depletes the pheromone and inhibits the return rate. We prove that the model is globally asymptotically stable in the absence of pheromone feedback. Then we show that pheromone feedback can lead to a loss of stability of the equilibrium and onset of sustained oscillations in the flow in and out of the nest via a Hopf bifurcation. This analysis sheds light on a potential key mechanism that enables arboreal turtle ants to effectively optimize their trail networks to minimize traveled path lengths and eliminate graph cycles.

I. INTRODUCTION

Oscillatory dynamics are a characteristic feature of computations in complex systems across nature and technology. For example, oscillations in the flow of nutrients and signaling molecules have been linked to the abilities of the cellular slime mold *Physarum polycephalum* to perform a variety of cognitive tasks, including shortest path computation [1]–[3]. Analogously, oscillations in nutrient and signaling molecule flow provide an active mechanism for regulating transport direction and coordinating resource allocation in fungal networks [4]. In distributed networks of neurons in the brain, oscillations are also fundamental for a wide range of functions including sensory and cognitive processing, memory, and the integration of neural activity [5]. In engineered systems, oscillatory or “spiking” control signals are being embraced as a design principle for generating flexible behaviors across neuromorphic hardware and robotics [6]–[10].

In this paper we study the onset of sustained oscillations in the flow into and out of the nest during foraging for the arboreal turtle ant *Cephalotes goniodontus* (henceforth referred to as turtle ant), in order to gain mechanistic insight into factors that enable turtle ant trail network optimization. To do this, we propose and analyze a compartmental model of turtle ant foraging dynamics. Turtle ants are known to maintain complex trail networks along tree branches and

leaves, connecting their nests and food sources [11], [12]. In recent work, it was shown that turtle ants can change these trail networks over time to minimize total traveled path length and to eliminate redundant graph features such as cycles [13], [14]. However, doing this requires the rate of flow of ants along trails to increase over time, which cannot be sustained indefinitely due to finite ant volume. Inspired by these findings, we will explore conditions under which sustained oscillations in the flow rate of turtle ants emerge from interactions between different groups of ants at the nest, and from feedback loops between the ants’ return rate to the nest and the pheromone concentration along their trails. Under oscillatory conditions, regular periods of flow rate growth that enable trail network optimization are followed by periods of flow rate decay. We conjecture that such oscillations may be a key feature of the distributed computation performed by turtle ants during foraging.

Mixed feedback is a key feature of oscillatory behavior [6], [7], [10]. In a mixed-feedback system, a positive feedback loop drives the state of a system away from equilibrium, while a negative feedback loop prevents these excitations from becoming unbounded. In this paper we introduce a dynamic model of turtle ant foraging in which there is mixed feedback between the ants’ flow between different behavioral compartments and the concentration of pheromone along their trails. We will show that this mixed feedback is key for explaining the emergence of sustained oscillations in the flow rate of ants entering and exiting a nest.

Previous work [13], [14] explored how the rate of pheromone deposition and the rate of pheromone decay allow the ants to maintain and repair a trail, showing that an increase in flow was necessary for smoothing out graph cycles. In this work, we build on these insights and explore a mechanistic explanation for *how* periodic increases in the flow might emerge. To do this we introduce the effect of unloading at the nest, which was not considered in previous work. Turtle ants forage for nectar and must unload it by trophallaxis (i.e. mouth-to-mouth transfer) to another ant at the nest. Our modeling incorporates the joint effects of unloading nectar and of pheromone feedback. We will show that together, these two effects can give rise to oscillations.

In our model, we differentiate between *trail ants* whose job it is to look for nectar and bring it back to the nest, and *nest ants* whose job it is to receive nectar from the returning foragers and bring it inside. We make a simplifying assumption that the foraging ants do not permanently return to the nest, and that nest ants do not go out to forage. To model interactions between trail ants and those that remain at the nest, we utilize a compartmental approach [15], also

A. Valentine is with the Center for Applied Mathematics at Cornell University, Ithaca, NY, 14850, av589@cornell.edu

D. M. Gordon is with the Department of Biology at Stanford University, Stanford, CA, 94305, dmrgordon@stanford.edu

A. Bizyaeva is with the Sibley School of Mechanical and Aerospace Engineering at Cornell University, Ithaca, NY, 14850, anastasiab@cornell.edu

common in the modeling of epidemics and other spreading processes [16], [17]. In our model, a trail ant supplying food must come into contact with a nest ant receiving food before it can return to the trails to forage. The competition between pheromone deposition by ants along their trail network and depletion of pheromone via evaporation is then a source of mixed feedback. Deposition is a source of positive feedback as it indirectly increases the rate of return of ants to the nest. On the other hand, evaporation is a source of negative feedback, since it depletes the pheromone and slows the rate of return. We will show that together, the effects of trophallaxis and of mixed pheromone feedback can destabilize the flow of ants and cause it to oscillate.

The following are the contributions of this paper. First, we introduce a new compartmental model that describes turtle ant foraging. Our model captures interactions between different groups of ants as they exchange food at the nest as well as a mixed feedback loop between the foraging ants' rate of return to the nest and the dynamics of the pheromone concentration along the trail. We prove that the model is well-posed. Second, we prove that in the absence of pheromone feedback the foraging model is globally asymptotically stable over its domain and find an explicit solution for the ant volumes in different behavioral compartments at the nest and on the trail at equilibrium. This result rules out the possibility of oscillatory flow rates from purely trophallaxis interactions. Third, we study the foraging model with pheromone feedback and derive implicit conditions for existence and uniqueness of an equilibrium solution. Numerically, we illustrate that this equilibrium can lose stability in a Hopf bifurcation. At the Hopf bifurcation there is an onset of sustained oscillations in the model, which we showcase in simulation. Together, these results highlight the central role of trophallaxis interactions, pheromone deposition, and mixed feedback in the optimization of turtle ant trail networks.

This paper is structured as follows. In Section II we state preliminaries. In Section III we motivate and introduce our foraging model. In Section IV we analyze the model with and without pheromone feedback, and present numerical studies. In Section V we conclude and discuss future work.

II. MATHEMATICAL PRELIMINARIES

Let $n \in \mathbb{N}$ and $S \subset \mathbb{R}^n$. The closure of S is $\bar{S} = \bigcap_{V \supset S, V \text{ closed}} V$. The interior of S is $S^\circ = \bigcup_{U \subset S, U \text{ open}} U$. The boundary of S is $\partial S = \bar{S} \setminus S^\circ$. The spectrum of $A \in M_{n \times n}(\mathbb{R})$, denoted $\text{spec}(A)$, is the set of eigenvalues of A . The spectral abscissa of A is $\sigma(A) = \max_{\lambda \in \text{spec}(A)} \{\text{Re}(\lambda)\}$.

A system of differential equations with continuous first derivatives on \mathbb{R}^n given by $\dot{x}_i = f_i(x_1, \dots, x_n) = f_i(x)$, $i \in \{1, \dots, n\}$, or equivalently $\dot{x} = f(x)$, with $f : \Gamma \mapsto \mathbb{R}^n$, $\Gamma \subseteq \mathbb{R}^n$ is called *competitive* if $\frac{\partial f_i}{\partial x_j} \leq 0 \forall i \neq j \forall x \in \Gamma$, and is called *cooperative* if $\frac{\partial f_i}{\partial x_j} \geq 0 \forall i \neq j \forall x \in \Gamma$.

Proposition II.1 (Flow of planar cooperative and competitive systems). [18, Theorem 2.3] Suppose $x \in \mathbb{R}^2$ and a system given by $\dot{x} = f(x)$ is competitive or cooperative. Suppose

$\Gamma = \mathbb{R}^2$ or \mathbb{R}_+^2 and let $y : [0, \infty) \mapsto \Gamma$ be the solution through $y(0)$. Then either $\|y(t)\| \rightarrow \infty$ or $y(t)$ converges to some point of $\bar{\Gamma}$ as $t \rightarrow \infty$.

III. MODEL SETUP

A. Compartmental Foraging Model

A colony of arboreal turtle ants occupies multiple nests along the trail network. In this paper we study the simplest scenario in which there is only a single nest. Consider two interacting groups of ants with $N > 0$ ants that remain at the nest and $M > 0$ ants that explore the trails. We assume that there are no transitions between these groups, i.e. that trail ants do not permanently return to the nest and that nest ants do not go out onto the trails. Under this assumption, the volumes N and M are constant.

Following a compartmental modeling paradigm [15], we observe that ants within both the nest and trail groups can be in one of two mutually exclusive behavioral states. The trail group is made up of \bar{F} forager ants out on the trails actively exploring for food and \bar{S} supplier ants that have acquired food and are waiting to hand it off to a nest ant. By conservation of volume, $\bar{F} + \bar{S} = M$. Analogously, we split the nest ant group into \bar{R} receiver ants picking up food from suppliers outside of the nest and \bar{I} interior ants that are inside of the nest, with $\bar{R} + \bar{I} = N$. Finally, we define normalized variables $R = \bar{R}/N, I = \bar{I}/N, F = \bar{F}/M, S = \bar{S}/M$ such that $R + I = 1$ and $S + F = 1$. Observe that R, S, I, F are each constrained to the unit interval $[0, 1]$.

Next, we consider transitions between the behavioral compartments within the nest and trail groups. We assume that foragers return to the nest to supply food at constant transition rate $\gamma > 0$, and interior ants become receivers at a transition rate $\alpha > 0$. To transition in the other direction, a supplier from the trail group must come in physical contact with a receiver from the nest group in order to hand off food. Therefore the transition rates from supplier back to forager, as well as those from receiver back to interior ant, will be state-dependent. By the law of mass action, the transition rate from \bar{R} to \bar{I} is $\beta \bar{S}/N$ with scaling parameter $\beta > 0$. Analogously, the transition rate from \bar{S} to \bar{F} is $\beta \bar{R}/M$. Assuming that the volume variables are continuous, observing that volume conservation implies $\dot{R} + \dot{I} = 0$, $\dot{S} + \dot{F} = 0$, and applying normalization, we arrive at a two-dimensional dynamical system that describes the dynamics of the nest and trail variables over time as

$$\dot{R} = \alpha(1 - R) - \beta \frac{M}{N} RS, \quad (1a)$$

$$\dot{S} = \gamma(1 - S) - \beta \frac{N}{M} RS. \quad (1b)$$

The variables $I(t)$ and $F(t)$ can be recovered from volume conservation as $I(t) = 1 - R(t)$ and $F(t) = 1 - S(t)$. Key features of (1) are summarized in Fig. 1.

B. Pheromone Feedback

The foraging model (1) accounts only for effects of direct interaction between ants. However, the ants' foraging dynamics are also coupled with and regulated by

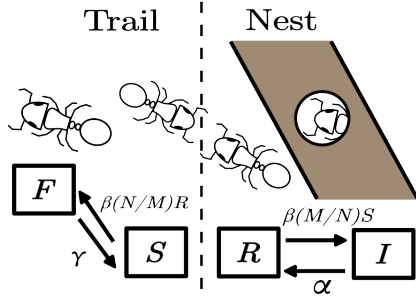


Fig. 1: Graphical summary of compartmental foraging model (1).

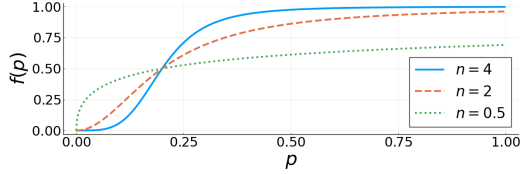


Fig. 2: Shape of the saturating Hill function $f(p) = \frac{k}{1+(p_0/p)^n}$ modeling the relationship between pheromone level and change in ant return rate for different choices of n . The other parameters of $f(p)$, k and p_0 are fixed at $k = 1, p_0 = 0.2$. In numerical simulations we used these values for k, p_0 , and chose $n = 4$.

the ants' pheromone deposition along trails. To model this coupling, we introduce a new dynamic variable $p \geq 0$ that represents pheromone concentration on the trail near the nest entrance. As ants move along the trail network, they deposit pheromone which increases the concentration p . The pheromone also evaporates at fixed rate $\mu > 0$, which decreases the concentration p . The rate of pheromone deposition is proportional both to the rate of return of foragers to supply food at the nest, captured by $\gamma\bar{F} = \gamma M(1 - S)$, and to the rate of return of suppliers to the foraging state, captured by $\beta\frac{R}{M}\bar{S} = \beta NRS$. An increase in either of these rates will increase the pheromone concentration p , since movement in either direction (towards or away from the nest) results in new pheromone deposition. We let $\nu > 0$ be a proportionality constant that tunes the deposition rate. Putting these pieces together, the temporal dynamics of the pheromone concentration p is governed by

$$\dot{p} = -\mu p + \nu(\gamma M(1 - S) + \beta NRS). \quad (2)$$

Next we consider the rate γ at which forager ants return to the nest to become suppliers. This rate was assumed to be constant in the baseline model (1). In reality, γ is closely related to the pheromone concentration p . Foragers rely on pheromone concentration to navigate the colony's trail networks. At high concentrations, pheromone is easy for foragers to detect, so navigating back to the nest to supply food is easier. At low concentrations, navigation becomes more difficult and the return rate of foragers will decrease as they may get lost or take a longer path towards food and back to the nest. To model this pheromone feedback, we take the return rate parameter γ to be dynamic, with dynamics

$$\tau_\gamma \dot{\gamma} = -\gamma + f(p) + \gamma_0, \quad (3)$$

where $f : \mathbb{R}^{\geq 0} \rightarrow \mathbb{R}^{\geq 0}$ a monotonically increasing function of p , $\tau_\gamma > 0$ a time scale, and $\gamma_0 \geq 0$ a base rate of return to the nest. In numerical simulations we choose f to be a saturating Hill function $f(p) = \frac{k}{1+(p_0/p)^n}$, with positive parameters k, p_0, n .

Together, our foraging model with pheromone feedback is a four-dimensional dynamical system given by (1), (2), and (3). The parameters of this model summarized in Table I. Note that the coupling between (2) and (3) is a source of mixed dynamic feedback in the model, as the evaporation of pheromone *inhibits* the rate of return while the deposition of pheromone *reinforces* the rate of return. Our analysis in Section IV will show that this mixed feedback is key to the emergence of limit cycles in the compartment variables, and therefore also in the flow rates of the groups. This hints at a key mechanism behind the ants' success at navigating trail networks, as a time-varying rate of flow along trails has previously been shown to play a key role in trail network optimization that enables ants to minimize traveled path lengths and eliminate cycles [14].

Parameter	Summary
N	Nest ant volume.
M	Trail ant volume.
α	Transition rate from interior to receiver at the nest.
β	Interaction rate scale between suppliers and receivers.
μ	Pheromone evaporation rate.
ν	Pheromone deposition rate.
γ_0	Base rate of γ , transition rate from forager to supplier; equal to γ in the 2d model (1).
τ_γ	Characteristic timescale of the response of the return rate γ to changes in pheromone concentration.
k	Scaling constant of $f(p)$
p_0	Saturation midpoint parameter of $f(p)$
n	Slope parameter of $f(p)$

TABLE I: Summary of model parameters in (1),(2),(3).

C. Well-Posedness

In the following Theorem we establish the well-posedness of the two-dimensional foraging model (1) and of its four-dimensional extension with pheromone feedback (2),(3) by proving that the variables R, S, p, γ do not take on values outside of the interpretable range under the flow of the dynamical system.

Theorem III.1. *The following statements hold.*

- 1) *The compact set $\Omega_1 = [0, 1] \times [0, 1]$ is positively invariant under the flow of (1) with static parameter $\gamma \geq 0$;*
- 2) *The set $\Omega_2 = [0, 1] \times [0, 1] \times \mathbb{R}^{\geq 0} \times \mathbb{R}^{\geq 0}$ is positively invariant under the flow of (1),(2),(3).*

Proof. 1) Let $\partial\Omega_1$ be the boundary of Ω_1 , which includes the sides and corners of the unit cube. If $R \in (0, 1), S = 0$, then $\dot{S} = \gamma > 0$. If $R \in (0, 1), S = 1$, then $\dot{S} = -\beta\frac{N}{M}R < 0$. If $R = 0, S \in (0, 1)$, then $\dot{R} = \alpha > 0$. If $R = 1, S \in (0, 1)$, then $\dot{R} = -\beta\frac{M}{N}S < 0$. If $R = S = 0$, then $\dot{R} = \alpha > 0, \dot{S} = \gamma > 0$. If $R = S = 1$, then $\dot{R} = -\beta\frac{M}{N} < 0, \dot{S} = -\beta\frac{N}{M} < 0$. If $R = 0, S = 1$, then $\dot{R} = \alpha > 0, \dot{S} = 0$. If $R = 1, S = 0$, then $\dot{R} = 0, \dot{S} = \gamma > 0$. With all of the cases

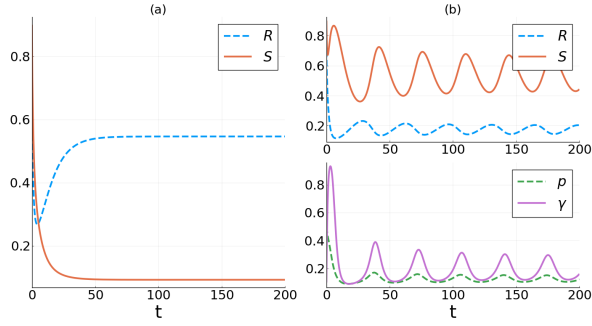


Fig. 3: (a) Numerically computed trajectory of (1) with parameters $N = M = 1, \alpha = 0.1, \beta = 0.9, \gamma = 0.05$ settling into the globally attracting equilibrium. (b) Numerically computed trajectory of (1),(2),(3) With the same parameters as in (a) and additionally $\mu = 0.6, \nu = 0.45, \tau_\gamma = 1, \gamma_0 = 0.05, k = 1, p_0 = 0.2, n = 4$ oscillating. The initial condition of (a) is $R(0) = 0.7, S(0) = 0.9$, R and S initial conditions in (a) and (b) are identical and $p(0) = 0.5, \gamma(0) = 0.1$ in (b).

checked, Nagumo's theorem [19, Theorem 4.7] implies Ω_1 is positively invariant.

2) We check that the flow along boundaries of Ω_2 does not exit the set. If $R \in [0, 1], S = 0, p, \gamma \in [0, \infty)$, then $\dot{S} = \gamma \geq 0$. If $R, S \in [0, 1], p = 0, \gamma \in [0, \infty)$, then $\dot{p} = \nu(\gamma M(1 - S) + \beta NRS) \geq 0$. If $R, S \in [0, 1], p \in [0, \infty), \gamma = 0$, then $\tau_\gamma \dot{\gamma} = f(p) + \gamma_0 > 0$. Other cases are consistent with 1). \square

IV. ANALYSIS

In this Section we study the foraging model (1),(2),(3), with the goal of classifying conditions under which oscillations in the compartment variables, and therefore in their rates of change, are possible.

A. Model without pheromone feedback

First we consider the compartmental foraging model (1) with a static interaction rate parameter γ . In the following Theorem we prove that under such static parameter assumptions, the model is globally asymptotically stable, i.e. oscillations are impossible.

Theorem IV.1 (Global Asymptotic Stability). *Consider (1) over $\Omega_1 = [0, 1] \times [0, 1]$.*

1) *The model has a unique fixed point $(R, S) = (R^*, S^*)$ in Ω_1 , given by $S^* = \frac{1}{2A}(A - B - 1 + \sqrt{(A - B - 1)^2 + 4AB})$, $R^* = B(1 - S^*)/S^*$ where $A = \gamma M^2/\alpha N^2$ and $B = \gamma M/\beta N$*

2) *(R^*, S^*) is globally attracting on Ω_1 .*

Proof. 1) At equilibrium, $\dot{R} = \dot{S} = 0$, which implies $\beta R^* S^* = \alpha \frac{N}{M}(1 - R^*) = \gamma \frac{M}{N}(1 - S^*)$. Solving this expression for R^* yields $R^* = 1 - A(1 - S^*)$, which can then be plugged into (1b) to arrive at a quadratic equation of the form $0 = A(S^*)^2 + (1 + B - A)S^* - B$ which has two solutions $S_\pm^* = \frac{1}{2A}(A - B - 1 \pm \sqrt{(A - B - 1)^2 + 4AB})$. These solutions generate $R_\pm^* = B \frac{1 - S_\pm^*}{S_\pm^*}$.

For compactness let $C_1 = A - B - 1$ and $C_2 = \sqrt{(A - B - 1)^2 + 4AB}$. Next, we will show that $R_-^*, S_-^* \notin$

Ω_1 . Observe that $C_2 > C_1$ for any $C_1 \in \mathbb{R}$ since $4AB > 0$. Then $C_1 - C_2 < 0$ which implies $S_-^* < 0$.

Finally, we will show that $(R_+^*, S_+^*) \in \Omega_1$. An analogous argument to above shows that $S_+^* > 0$. Suppose $S_+^* < 1$. Then $(1 + B - A)^2 + 4AB < (A + B + 1)^2$. Expanding and canceling like terms results in the condition $0 < 2A$ which is always satisfied, so $S_+^* < 1$. $R_+^* = B \frac{1 - S_+^*}{S_+^*}$ implies $R_+^* > 0$ since $S_+^* \in (0, 1)$. Finally, suppose $R_+^* < 1$. Writing this in terms of S_+^* gives $B \frac{1 - S_+^*}{S_+^*} < 1$ which rearranges to $S_+^* > \frac{B}{1+B}$. Substituting our expression for S_+^* , multiplying by $2A$, and rearranging yields $\sqrt{(A + B - A)^2 + 4AB} > \frac{2AB}{1+B} + 1 + B - A$, which simplifies to $A > 0$ which is always true, so $R_+^* < 1$. The equilibrium $(R^*, S^*) = (R_+^*, S_+^*)$ is therefore unique in Ω_1 .

2) The Jacobian of (3) is:

$$J(R, S) = \begin{bmatrix} -\alpha - \beta \frac{M}{N} S & -\beta \frac{M}{N} R \\ -\beta \frac{N}{M} S & -\gamma - \beta \frac{N}{M} R \end{bmatrix}$$

Since $S, R \in [0, 1]$, all entries of J are non-positive, and the system given by (1) is *competitive*. The dynamics are 2-dimensional, and by Proposition II.1, any trajectory $(R(t), S(t))$ starting from initial condition $(R(0), S(0)) \in \Omega_1$ will either approach an equilibrium or $\|(R(t), S(t))\| \rightarrow \infty$ as $t \rightarrow \infty$. By Theorem III.1, the bounded region Ω_1 is invariant under the flow of (1), which means all trajectories must settle to an equilibrium. Since the equilibrium (R^*, S^*) defined in part 1) of this theorem is unique in Ω_1 , we conclude it must be globally asymptotically stable. \square

A numerical simulation of the foraging model (1) settling to its unique globally asymptotically stable equilibrium described in Theorem IV.1 is shown in Fig. 3(a).

B. Full model

Theorem IV.1 implies that physical interactions between ants during trophallaxis are not sufficient to cause oscillations in the model. An additional mechanism is necessary in order to destabilize the equilibrium and cause such oscillations. In this Section we explore the pheromone feedback (3), (2) as a possible mechanism that could drive this loss of stability. First, we establish conditions for existence and uniqueness of an equilibrium in the full model. Next, we numerically study the stability of this equilibrium, focusing on the effects of variations in transition rate parameters α and β . We will show that for a range of these parameters, the equilibrium becomes unstable. At the onset of this instability, the model undergoes a Hopf bifurcation, and oscillations emerge.

First, in the following Theorem, we derive conditions for existence and uniqueness of an equilibrium for the full foraging model with dynamic pheromone feedback.

Theorem IV.2 (Equilibrium Existence and Uniqueness). *Equilibria $(S, R, p, \gamma) = (S^*, R^*, p^*, \gamma^*)$ of the model (1), (2), (3) are implicitly defined by $S^* = \frac{\alpha N}{\beta M} \frac{(1 - R^*)}{R^*}$, $p^* = 2 \frac{\nu}{\mu} \alpha \frac{N^2}{M} (1 - R^*)$, $\gamma^* = f\left(2 \frac{\nu}{\mu} \alpha \frac{N^2}{M} (1 - R^*)\right) + \gamma_0 = \alpha \beta \frac{N^2}{M} \frac{R^* (1 - R^*)}{\beta M R^* - \alpha N (1 - R^*)}$, where R^* is a root of this implicit*

relationship in the unit interval $[0, 1]$. At least one equilibrium exists in Ω_2 for all parameter values. Furthermore, any $R^* \in \left(\frac{\alpha N}{\alpha N + \beta M}, 1\right)$. Let R_1 be the first value of $x \in \left(\frac{\alpha N}{\alpha N + \beta M}, 1\right)$ satisfying the equilibrium conditions. Then if $\int_{R_1}^1 f' \left(2\frac{\nu}{\mu} \alpha \frac{N^2}{M} (1-x)\right) - \frac{1}{2} \frac{\nu}{\mu} \beta \frac{\alpha N (1-x)^2 + \beta M x^2}{(\alpha N (1-x) + \beta M x)^2} dx > 0$, then the implicit relationship above defines a unique equilibrium $(S^*, R^*, p^*, \gamma^*)$ in Ω_2 where $R^* = R_1$.

Proof. At an equilibrium, the right hand side of (1a), (1b), (2), (3) is equal to zero. We will use these relationships to find expressions for S^*, γ^*, p^* as a function of R^* , and an implicit function whose zeros define the values of R^* at steady state. From (1a) and (1b) we see that $\gamma^*(1-S^*)M = \alpha(1-R^*)\frac{N^2}{M}$. Plugging this in to (2) to eliminate S^* we obtain $p^* = 2\frac{\nu}{\mu} \alpha \frac{N^2}{M} (1-R^*)$. Then (1a) implies $S^* = \frac{\alpha N}{\beta M} \frac{(1-R^*)}{R^*}$. To obtain an implicit equation for R^* , we can notice that (1b) gives $\gamma^* = \beta \frac{N}{M} \frac{R^* S^*}{1-S^*} = \frac{\frac{N^2}{M^2} \alpha R^* \left(\frac{1-R^*}{\beta M R^*}\right)}{1 - \frac{\alpha N (1-R^*)}{\beta M R^*}} = \frac{N^2}{M} \alpha \beta \frac{R^* (1-R^*)}{\beta M R^* - \alpha N (1-R^*)} := g(R^*)$, while (3) gives $\gamma^* = f(p^*) + \gamma_0 = f\left(2\frac{\nu}{\mu} \alpha \frac{N^2}{M} (1-R^*)\right) + \gamma_0 := h(R^*)$. Setting these two expression for γ^* equal to each other gives our implicit equation for R^* .

To prove existence and uniqueness of these solutions, we study the number of intersections between the functions $h(x)$ and $g(x)$ over the unit interval $x \in [0, 1]$, since the zeros of $h(R^*) - g(R^*) = 0$ generate the equilibria of the model. First, observe that $h(0) = \gamma_0$, $h(1) = \frac{k}{1+p_0^2} + \gamma_0$, $g(0) = 0$, and $g(1) = 0$. The function $h(x)$ is continuous and monotonically decreasing on $[0, 1]$, so $\gamma_0 \leq h(x) \leq \frac{k}{1+p_0^2} + \gamma_0$. The function $g(x)$ has a discontinuity at $x = \frac{\alpha N}{\alpha N + \beta M}$ where its denominator is zero. Everywhere else in the set interior $(0, 1)$, $g(x)$ is continuous and differentiable, with derivative

$$g'(x) = -\alpha \beta \frac{N^2}{M} \frac{\beta M x^2 + \alpha N (1-x)^2}{(\alpha N (1-x) + \beta M x)^2} < 0.$$

Since $g(0) = 0$, $\lim_{x \rightarrow \left(\frac{\alpha N}{\alpha N + \beta M}\right)^-} g(x) = -\infty$, and $g'(x) < 0$ for all $x \in \left(0, \frac{\alpha N}{\alpha N + \beta M}\right)$, we conclude that over this interval, $g(x) < 0$ while $h(x) > 0$ and intersections are impossible, which rules out equilibria in this region.

Next, we consider the interval $x \in \left(\frac{\alpha N}{\alpha N + \beta M}, 1\right)$. Observe that $\lim_{x \rightarrow \left(\frac{\alpha N}{\alpha N + \beta M}\right)^+} g(x) = \infty$. Since $g(1) = 0$, we see that $h(1) - g(1) = \frac{k}{1+p_0^2} + \gamma_0 > 0$. Since $h(x)$ is bounded on the unit interval, $\lim_{x \rightarrow \left(\frac{\alpha N}{\alpha N + \beta M}\right)^+} h(x) - g(x) = -\infty$. Then by the intermediate value theorem, there must exist at least one value $x = R^*$ at which $h(R^*) = g(R^*)$. This establishes existence of an equilibrium in this interval. This equilibrium is unique if the difference $h(x) - g(x)$ does not cross zero a second time. The integral condition in the Theorem statement imposes this non-intersection. \square

Theorem IV.2 establishes that the model (1),(2),(3) always has at least one equilibrium. Furthermore, under mild assumptions about the shape of the function $f(p)$ that defines

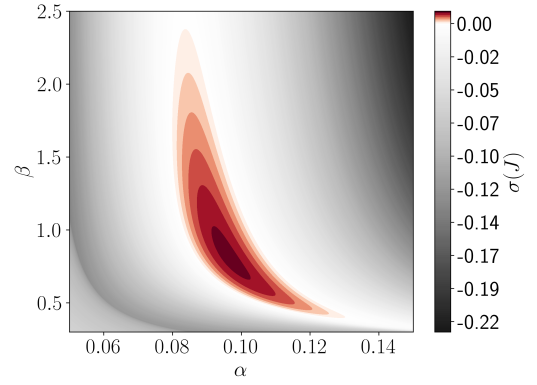


Fig. 4: Contour plot of the spectral abscissa of the Jacobian of 4 for a range of α and β . Computed for 1000 different values of α and β over a uniform grid, with $\alpha \in [0.05, 0.15]$ and $\beta \in [0.3, 2.5]$, for a total of 10^6 grid points. The rest of the model parameters are as in Fig. 3. Oscillations occur in the red region where $\sigma(J) \geq 0$.

the relationship between the pheromone concentration and the ants' return rate to the nest, this equilibrium is unique. Next, we study the stability of this equilibrium. The Jacobian $J(S^*, R^*, p^*, \gamma^*)$ of the model evaluated at its equilibrium is given by the matrix

$$\begin{bmatrix} -\alpha - \beta \frac{M}{N} S^* & -\beta \frac{M}{N} R^* & 0 & 0 \\ -\beta \frac{N}{M} S^* & -\gamma^* - \beta \frac{N}{M} R^* & 0 & 1 - S^* \\ \nu \beta \frac{N}{M} S^* & \nu(-\gamma^* M + \beta N R^*) & -\mu & \nu M (1 - S^*) \\ 0 & 0 & \frac{f'(p^*)}{\tau_\gamma} & -\frac{1}{\tau_\gamma} \end{bmatrix} \quad (4)$$

where R^*, S^*, p^*, γ^* are uniquely defined by a given choice of model parameters via the implicit relationship derived in Theorem IV.2, provided the stated uniqueness condition is satisfied. When all eigenvalues of (4) have negative real part, the equilibrium is locally exponentially stable.

A common parametrized path to oscillation in a dynamical system is via a Hopf bifurcation [20, Theorem 3.4.2]. In a Hopf bifurcation, as a parameter is varied, an equilibrium loses stability and two complex conjugate eigenvalues of its Jacobian simultaneously cross the imaginary axis. At the onset of this instability, oscillations emerge. To find such regions of instability we study numerically the spectral abscissa of the Jacobian (4) for the choice of model parameters $N = M = 1$, $\gamma_0 = 0.05$, $k = 1$, $p_0 = 0.2$, $n = 4$, $\mu = 0.6$, $\nu = 0.45$. The parameters α and β are left as free parameters. This choice of parameters satisfied the conditions for equilibrium uniqueness of Theorem IV.2.

We numerically solve the implicit equations derived in Theorem IV.2 to find the model equilibrium over a grid of α , β , and then evaluate the eigenvalues of the Jacobian (4) at each parametrized equilibrium. The result of this numerical study is shown in Fig. 4. The parameter values in the gray region of the plot correspond to regions of local stability for the equilibrium. Inside of the red region, the equilibrium is unstable and the Jacobian has a leading pair of complex conjugate eigenvalues. The boundary of the red region corresponds to Hopf bifurcation points, crossing which by varying α and/or β from the region exterior into the

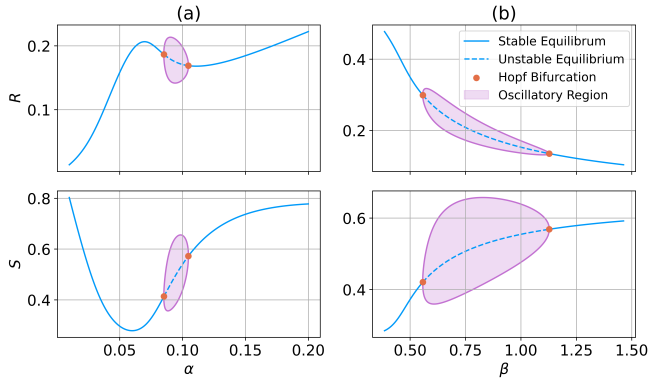


Fig. 5: Numerical Continuation of (1),(2),(3), computed with the Julia package BifurcationKit.jl [21] in parameters α (column (a)) and β (column (b)), plotted with respect to R and S . The vertical width of the oscillatory region at a fixed parameter value corresponds to the range of the limit cycle. Parameters not listed in the plot are same as in Fig. 3.

interior leads to loss of stability and emergence of oscillation. A simulation of a representative oscillation in this region is shown in Fig. 3(b). Finally, we further confirm the onset of oscillation over a localized region in α and β by computing bifurcation diagrams using numerical continuation software. We fix one of the parameters α , β and vary the second to compute solution branches and bifurcation points, see Fig. 5. Together these numerical results confirm the existence of parameter regimes in which the flow of ants into and out of the nest oscillates and suggests a mechanistic principle leveraged by turtle ants to enable effective trail optimization.

V. DISCUSSION AND FUTURE WORK

In this work we proposed and analyzed a mechanistic model of turtle ant foraging dynamics to explore onset of oscillations in the flow into and out of a nest. We showed that trophallaxis interactions between ants at the nest alone are not enough to induce oscillations in their flow. However when these interactions are considered in combination with dynamic pheromone feedback, oscillations become possible. Our numerical studies reveal a localized region in the (α, β) parameter space in which the flow oscillates. Interestingly, we see that the oscillation persists for a wider range of β while small variations in α can push the system out of the oscillatory regime. The transition rates α and β are measurable in field experiments, which means that our model-based analytic insights can be tested against real-world observations of turtle ants.

In future work, we will extend our modeling by relaxing the simplifying assumption made in this paper that trail ants do not permanently return to the nest, and that nest ants do not go out to forage. We will consider the effects of transitions between nest and trail ants to derive a more general set of conditions for oscillation onset. Furthermore, we plan to expand our modeling to consider multiple nests to understand effects of expanding the trail network on the properties of the emergent oscillation. Our ultimate goal with this research effort is to generate a set of model-based

testable hypotheses that can be compared against field data and can be used to design future experiments. This work will provide new insights into the role of oscillations in decentralized computation in nature.

REFERENCES

- [1] A. Boussard, A. Fessel, C. Oettmeier, L. Briard, H.-G. Döbereiner, and A. Dussutour, "Adaptive behaviour and learning in slime moulds: the role of oscillations," *Philosophical Transactions of the Royal Society B*, vol. 376, no. 1820, p. 20190757, 2021.
- [2] A. Dussutour and C. Arson, "Flow-network adaptation and behavior in slime molds," *Fungal Ecology*, vol. 68, p. 101325, 2024.
- [3] L. Gyllingberg, Y. Tian, and D. J. Sumpter, "A minimal model of cognition based on oscillatory and reinforcement processes," *arXiv preprint arXiv:2402.02520*, 2024.
- [4] S. S. Schmieder, C. E. Stanley, A. Rzeplia, D. van Swaay, J. Sabotić, S. F. Nørrelykke, A. J. deMello, M. Aebi, and M. Künzler, "Bidirectional propagation of signals and nutrients in fungal networks via specialized hyphae," *Current Biology*, vol. 29, no. 2, pp. 217–228, 2019.
- [5] E. Başar, C. Başar-Eroğlu, S. Karakaş, and M. Schürmann, "Brain oscillations in perception and memory," *International journal of psychophysiology*, vol. 35, no. 2-3, pp. 95–124, 2000.
- [6] R. Sepulchre, G. Drion, and A. Franci, "Control across scales by positive and negative feedback," *Annual Review of Control, Robotics, and Autonomous Systems*, vol. 2, no. 1, pp. 89–113, 2019.
- [7] —, "Excitable behaviors," *Emerging Applications of Control and Systems Theory: A Festschrift in Honor of Mathukumalli Vidyasagar*, pp. 269–280, 2018.
- [8] R. Sepulchre, "Spiking control systems," *Proceedings of the IEEE*, vol. 110, no. 5, pp. 577–589, 2022.
- [9] C. Cathcart, I. X. Belaustegui, A. Franci, and N. E. Leonard, "Spiking nonlinear opinion dynamics (S-NOD) for agile decision-making," *IEEE Control Systems Letters*, 2024.
- [10] O. Juarez-Alvarez and A. Franci, "Collective rhythm design in coupled mixed-feedback systems through dominance and bifurcations," *IEEE Transactions on Control of Network Systems*, pp. 1–12, 2025.
- [11] D. M. Gordon, "The dynamics of foraging trails in the tropical arboreal ant *Cephalotes goniodontus*," *PLoS One*, vol. 7, no. 11, p. e50472, 2012.
- [12] —, "Local regulation of trail networks of the arboreal turtle ant, *Cephalotes goniodontus*," *The American Naturalist*, vol. 190, no. 6, pp. E156–E169, 2017.
- [13] A. Chandrasekhar, J. A. Marshall, C. Austin, S. Navlakha, and D. M. Gordon, "Better tired than lost: Turtle ant trail networks favor coherence over short edges," *PLoS computational biology*, vol. 17, no. 10, p. e1009523, 2021.
- [14] S. Garg, K. Shiragur, D. M. Gordon, and M. Charikar, "Distributed algorithms from arboreal ants for the shortest path problem," *Proceedings of the National Academy of Sciences*, vol. 120, no. 6, p. e2207959120, 2023.
- [15] D. Sumpter and S. Pratt, "A modelling framework for understanding social insect foraging," *Behavioral Ecology and Sociobiology*, vol. 53, pp. 131–144, 2003.
- [16] F. Brauer, "Compartmental models in epidemiology," *Mathematical epidemiology*, pp. 19–79, 2008.
- [17] S. Gracy, P. E. Paré, J. Liu, H. Sandberg, C. L. Beck, K. H. Johansson, and T. Başar, "Modeling and analysis of a coupled SIS bi-virus model," *Automatica*, vol. 171, p. 111937, 2025.
- [18] M. W. Hirsch, "Systems of differential equations which are competitive or cooperative: I. limit sets," *SIAM Journal on Mathematical Analysis*, vol. 13, no. 2, pp. 167–179, 1982. [Online]. Available: <https://doi.org/10.1137/0513013>
- [19] F. Blanchini, S. Miani *et al.*, *Set-theoretic methods in control*. Springer, 2008, vol. 78.
- [20] J. Guckenheimer and P. Holmes, *Nonlinear oscillations, dynamical systems, and bifurcations of vector fields*. Springer Science & Business Media, 2013, vol. 42.
- [21] R. Veltz, "BifurcationKit.jl," Jul. 2020. [Online]. Available: <https://hal.archives-ouvertes.fr/hal-02902346>